applied sciences

MDPI

Article

A Predictive Reliability Model to Assess the Performance of Photovoltaic Systems

Nahed Solouma [1,*] and Amal El Berry [2]

[1] BME Department, College of Engineering, King Faisal University, Hufof 3959-36362, Saudi Arabia
[2] Mechanical Engineering Department, Engineering and Renewable Energy Research Institute, National Research Centre (NRC), Cairo 12622, Egypt; amalelberry@yahoo.com
* Correspondence: nsolouma@kfu.edu.sa; Tel.: +966-13-589-7746

Abstract: Clean energy is extremely important not only because of economic purposes but also for health considerations. The use of photovoltaic (PV) systems is growing, with the increased needs for electricity. This requires more attention to research of PV systems. In this study, a method to predict the expected lifetime based on the reliability of system performance is proposed. Geographical data were collected near two different locations: Cairo, Egypt and Riyadh, Saudi Arabia. The PV system was simulated with inputs from collected data to obtain the device factors and system responses. To study the significance of inputs and device parameters on the system responses, the Taguchi OA method was used. The probability density function (pdf) of the time of acceptable performance was estimated from the simulation data. A reliability analysis method was applied to the obtained pdf to estimate the reliability function, lifetime or mean life, reliable life, and rate of failure of the used PV system as assessment factors. The results showed that the system efficiency is highly dependent on the ambient temperature, while the performance ratio depends on many variables. The reliability analysis revealed that the field orientation of 30° tilt and 20° azimuth and of 30° tilt and 30° azimuth are best for near Cairo and near Riyadh, respectively. These orientations lead to the longest mean life of 772.25 and 688.36 months for Cairo and Riyadh, respectively. It also resulted in the lowest failure rates of 0.001295 and 0.001228 per month for both regions.

Keywords: PV systems; reliability; performance analysis; Taguchi OA design

check for updates

Citation: Solouma, N.; El Berry, A. A Predictive Reliability Model to Assess the Performance of Photovoltaic Systems. *Appl. Sci.* **2022**, *12*, 2885. https://doi.org/10.3390/app12062885

Academic Editor: Gaetano Zizzo

Received: 10 February 2022
Accepted: 8 March 2022
Published: 11 March 2022

Publisher's Note: MDPI stays neutral with regard to jurisdictional claims in published maps and institutional affiliations.

Copyright: © 2022 by the authors. Licensee MDPI, Basel, Switzerland. This article is an open access article distributed under the terms and conditions of the Creative Commons Attribution (CC BY) license (https://creativecommons.org/licenses/by/4.0/).

1. Introduction

Renewable clean energy has been the interest of many researchers because of its positive impact on the world. On top of these positive impacts, clean energy usage does not generate pollution or harmful gasses. This helps save humans and wildlife in general. In addition, clean energy production is more economical compared to those requiring oil transport and refining. Moreover, the sources of clean energy are diverse and somehow persistent, minimizing the dependence on other countries [1]. Many sources of renewable energy have been investigated such as solar energy, wind energy, and others. Solar power as a renewable, sustainable and clean energy source is foreseen to be the dominant source of electricity in the future. The worldwide growing population and the industrial development have resulted in a continuous increase in the countries' demands for electricity [2]. Meanwhile, about 40–50% of the total generated electricity is consumed by the residential sector [3,4]. Researchers have been placing more efforts to study and improve the performance of photovoltaic systems as a solar energy harvesting technology [5]. Solar radiation is the input of the photovoltaic systems, and electric power is their output, with many parameters affecting the performance and efficiency of the systems. Collecting and analyzing the input, parameters, and output data of such systems is important to study to improve their responses.

The amount of global solar radiation is essential for the optimum design of solar energy systems, especially for PV systems. As the effect of solar radiation varies with the

orientation of the PV system, it is important to study the performance of the PV systems at different orientations for a specific geographical region of the world. This can help estimate the best system alignment to obtain optimum system performance [6].

Generally speaking, the PV cell is a transducer that converts solar (optical) energy into electrical energy. Utilizing the PV cells for power production requires more parts to form a PV system. Studying such systems can be achieved through their transfer function or by collecting and analyzing data about operational conditions, inputs, outputs of different parts of the device (device factors), and system responses. Different settings can be considered to collect data from different experiments. The following sections give brief explanations of such data components and models.

1.1. The Operational Conditions

These include the atmospheric conditions and the field orientation parameters. The atmospheric conditions include the ambient temperature T_A, the velocity of wind V_w and the global horizontal solar radiation, or shortly, the global horizontal irradiation. While the atmospheric conditions are determined by the location of the system on Earth, the parameters of field orientation can be adjusted for optimum performance. There are two parameters for the field orientation: tilt angle of the PV plane β and its azimuth angle α_z. These two parameters affect the amount of solar energy collected by the system. According to [7], the three parameters zenithal angle θ_z, azimuth angle α_z and altitude define the solar coordinates. The zenith angle θ_z is the angle of incidence of a beam from the sun on a horizontal plane, which is the angle between the vertical direction and the line to the sun.

The azimuth angle α_z is defined as the angular displacement on the horizontal plan taken from south of the projection of the beam radiation [7]. This angle is given by:

$$\alpha_z = arcsin\ (cos(\delta)sin(H)/cos(h))$$

where,

- h is the solar altitude angle which is the complement of θ_z;
- H is the hour angle, defined as the angular displacement that the local meridian makes by a rate of 15° per hour—either east or west due to the rotation of the Earth. According to [7], H is negative in the morning and positive in the afternoon and given by:
$$H = 15^\circ\ (RTS - 12)$$
- RTS is the real time system in hours and is counted from 0 to 24 h;
- δ is the declination angle. In [8], δ is defined as the angle that the rays make with the equator plane of the Earth for a specified day number n and is given by:
$$\delta = 23.45\ sin\left[360 * \frac{284 + n}{365.25}\right]$$

1.2. Inputs of the PV System

The input to the PV system is the part of the global horizontal radiation that is incident on the panels and is assumed to be converted into electrical energy. This radiation is called global incident radiation G_i, and is measured in kWh/m^2. The global incident radiation depends on the global horizontal radiation G_h, which is composed of two components, according to [9], as follows:

$$G_h = D_h + B_h$$

where B_h and D_h are the diffuse and direct beam horizontal radiations in kWh/m^2. The direct beam horizontal irradiation B_h is the radiation that reaches the Earth and that comes from a beam traveling directly from the sun to the Earth without any atmospheric scattering [9]. Conversely, the diffuse horizontal radiation D_h is the sun radiation that has

been scattered by particles and molecules of the atmosphere but finally reaches the Earth's surface [9]. These variables are meteorological data available in the databases.

The global horizontal incident radiation G_i is defined as the amount of global solar radiation incident on the collector plane and is related to the field orientation parameters B_h and D_h by the following relation:

$$G_i = \frac{cos(\theta_i)}{cos(\theta_Z)} B_h + \frac{(1 + \cos(\beta))}{2} D_h \quad (1)$$

where the angle of incidence θ_i and θ_Z are evaluated geometrically by the direction of the plane to the sun (declination, latitude, hour angle) and the field orientation (β, α_z) of the used PV plane.

The effective global radiation incident on the collector (G_{eff}) is related to G_i after correction for optical losses due to shades and soiling. Thus, it is considered as an input instead of G_i, to take the optical losses into consideration.

1.3. The Device Factors

The device factors are the technical specifications of the array and battery. These factors might differ from one model to another and indicate the quality of the PV system. The following is a list of the important device factors:

1. Array efficiency η_{arr}: this is defined as the energy at the array output relative to the irradiance on the total area of the collector and given by:

$$\eta_{arr} = \frac{E_{arr1}}{G_i} \quad (2)$$

   where E_{arr1} is the energy produced at the output of the array, in one hour, while the battery is charging.
2. The array performance ratio APR: this is defined by the array yield to the reference yield as:

$$APR = \frac{Y_a}{Y_r} \quad (3)$$

   where Y_r is the reference yield of the system in kWh/m^2/day, which is the amount of energy received by the array collector in one day, and Y_a is the array yield or the daily production of the array in kWh/kWp/day. The unit kWh/kWp means the produced electrical energy from the rough area of the array, so, there is no conflict in units of Y_r and Y_a.

1.4. Output and System Responses

The output is the produced energy E_{prod} is available for usage and backup while the array is producing. This energy is given by:

$$E_{prod} = E_{arr} - E_{lost} + E_{full}$$

where E_{arr} is the energy at the output of the array while the battery is charging, E_{lost} is the energy losses due to conversion and wiring, and E_{full} is the unused energy due to full-battery loss.

The system responses are the specs used to assess the system and include:

1. System efficiency η: the ratio of the produced energy to the irradiance on the total area of the collector and given by:

$$\eta = \frac{E_{prod}}{G_i}$$

2. System performance ratio (PR): the ratio of the produced energy to the energy that would be produced if the system is continuously working at its nominal STC efficiency. The performance ratio is also given by the ratio of the system yield to the reference yield. This ratio indicates the quality of the system regardless of the incident irradiance.

The PV system was analyzed and assessed using different methods. Among these methods are the artificial neural networks (ANN), the adaptive neuro-fuzzy inference system (ANFIS), and others mentioned below for review. In this work, the PV system performance was analyzed by the reliability of this performance. Although reliability engineering is a famous and robust technique, it is not found in the literature. The aim of this study is to predict some measurements based on the system functionality to be used for optimum settings and system assessment.

Ravi et al. [6] suggested an approach to maximize the total number of solar panels in a PV system in a given area without compromising the overall system efficiency, while also enhancing the output energy. The authors of this work achieved this by optimizing the installation parameters such as pitch, tilt angle, altitude angle, shading and gain factor, aiming to improve energy yield.

In [10], the authors studied the effects of using a system for sun tracking of multi-axis type on electrical generation to evaluate its performance. The authors of this work investigated the effects of tilt angles and azimuth on the output power of a PV module. They estimated the instantaneous increments of the generated power when the PV module is mounted on a single- and dual-axis tracking system. The results they obtained showed that the yearly optimal tilt angle of a fixed panel facing the south is approximately 0.9 times the latitude of the city they considered.

The slope of the panels of a photovoltaic system was studied in [11] for three cities. They utilized the Liu and Jordan model to obtain the monthly optimal angle of tilt. The results they obtained showed that the optimal tilt angle for these cities is less than 5°.

Optimizing the performance of a model based on an artificial neural network to estimate the solar radiation in the eastern region of Turkey is provided in [12]. They discussed the estimation of performance by different types of neural networks. The work of these authors aimed to evaluate the use of a neural network for such an optimization problem.

A code-based modeling approach was proposed in [13] to help study PV technologies. The authors used a synthesized dataset for the coding and training of the model. They used commercial PV modules to validate the model they suggested. Using this model, they repeatedly and reliably predicted the maximum power point, short circuit current and open circuit voltage with <2%, 0%, and <10% deviations, respectively.

In [14], Kasra et al. proposed an ANFIS (adaptive neuro-fuzzy inference system) to identify the most significant parameters to predict the daily global solar radiation. The ANFIS is a process to select variable input parameters with 1, 2 and 3 inputs to identify the most significant sets for three cases. They used nine variables of the duration of sunshine (n), (N) as the maximum of (n), maximum, minimum and average ambient temperatures, water vapor pressure (VP), relative humidity (Rh), extraterrestrial radiation (Ho) and sea level pressure (P). The results they obtained showed that the optimum sets of inputs differed from one city to another due to different solar radiation and climate conditions.

Preemalatha et al. [15] developed an artificial neural network (ANN) model to predict solar radiation. They used meteorological data for the previous 10 years from databases of different locations. The ANN model they used is based on root mean square error (RMSE), minimum mean absolute error (MAE), and maximum linear correlation coefficient (R). The authors of this work confirmed the accuracy of this ANN model to predict the monthly average global radiation.

An efficient ANN model was proposed in [16] to predict photovoltaic power. They used different learning algorithms and training data from different databases to predict the power production one day ahead with short computational time. The results they obtained showed an enhancement of up to 1%, 1.5% and 15% for the MAE (mean absolute

error), R^2 (coefficient of determination) and RMSE (root mean square error) as performance metrics, respectively.

In [17], an optimization technique based on a genetic algorithm and wavelet ANN was provided to forecast the daily solar radiation. They used the genetic algorithm to optimize the weights inputs, outputs, translation factors and scale factors. The daily radiation data, cleanness index and temperature were used for training the ANN using the gradient descent method. They obtained satisfactory results for the daily solar radiation.

Statistical regression techniques were suggested in [18] to demonstrate the robustness of the day of the year-based models for solar radiation prediction. The authors evaluated the performance of the selected models by analyzing different statistical indicators.

This paper is organized as follows: An introduction to the PV system with a brief review is given in Section 1. The proposed methodology and used materials are described in Section 2. The results are presented and discussed in Section 3. At the end of this paper, the work is concluded.

2. Materials and Methods

The data used in this work were collected from two different geographical regions as described:

- near Cairo: Cairo International Airport, Egypt, time zone UT + 2 with latitude 30.13° N, longitude 31.40° E and altitude 36 m;
- near Riyadh: Al Ahsa, Saudi Arabia, time zone UT + 3 with latitude 22.0° N, longitude 51.0° E and altitude 138 m.

Three experiments were run with both datasets at different settings of field orientation tilt angle β and azimuth angles α_z. These settings were determined to include the most common values of (β and α_z) used in both regions as follows:

1. Experiment 1 at (30° and 0°);
2. Experiment 2 at (30° and 20°);
3. Experiment 3 at (30° and 30°).

The values of the meteorological data (T_A, V_w, G_i) were collected from the available database of both regions. These data cover the twelve months of the year.

The method proposed to predict the assessment measures and lifetime, or the time over which the system can work properly, is composed of the following three major steps, which are described in later subsections.

1. Simulation of the PV system;
2. Factorial design experiments;
3. Reliability analysis.

2.1. Simulation of the PV System

In this major step, the performance of the photovoltaic system was simulated considering the values of inputs and operational conditions of both regions. The simulation results in the corresponding values of the device factors and system responses. For this study, the specialized software called PVsyst (version 7) was used to simulate the work of the PV system with the following specifications:

- System type: unlimited sheds;
- PV array of 308 PV modules (model *ET-P660_255WWCO Maxim*);
- The inverter pack is composed of 44 inverters (model *CSI-1.5KTL1P-GI-FL*).

By default, this simulation software considers a redundant number of variables for input and calculates a redundant number of device factors and the three system responses. For this study, we considered the most discriminable variables and factors to eliminate the redundancy. An example is that the simulation software calculates Y_a, APR and η_{arr} among other variables. From these three variables, we considered only the array yield Y_a, as it indicates the values of APR and η_{arr}.

2.2. Factors Design Experiments

In this major step, an experiment was designed to study the significance of the inputs and device factors were selected as variables affecting the output and system responses and hence its quality. This gives an overview of the impact of each individual variable of which field orientation allows for the best utilization of global irradiation.

To achieve this task, we applied the robust Taguchi Orthogonal Array (Taguchi OA) for factorial design.

The Taguchi OA technique is a full factorial design (FFD) of experiments. This highly fractional design can consider a selected subset of factor (including inputs and device factors) runs at different levels of values. The balanced performance of the orthogonal arrays ensures equal consideration of all factors at all levels. Thus, individual factors can be evaluated independently of each other regardless of the design fractionality [19].

In this work, the significance and effects of the four factors (T_A, V_w, G_{eff}, Y_a) on the output and the two system responses (E_{prod}, η, PR) were estimated using the full factorial Taguchi OA design. The reason for using these four factors is to consider all factors that affect the system performance. In more detail, the weather-related factors and device factors that affect the system performance must be considered, but redundancy should be avoided. T_A, V_w and G_i are the weather-related factors that affect performance. T_A and V_w are explicitly considered. The reason for using G_{eff} is that it implicitly includes the G_i as well as the effect of optical losses. The same concept was utilized when using Y_a, as it implicitly includes other device factors APR and Y_r as per the definitions mentioned in section number 1.

The software DOE++ is used for a 2-level full factorial Taguchi OA. The settings used for the 6 experiments (3 field orientations and 2 datasets) are shown in Tables 1 and 2 for near Cairo and near Riyadh, respectively. In these tables, L12 means the number of runs equal to 12 (as the length of data collected over the 12 months of the year). The value 2^10 indicates that the Taguchi OA algorithm was applied for 2 levels (low and high) with 10 output terms in the equations describing the responses. The 10 output terms are related to the 4 factors and their 6 combinations for 2 locations.

Table 1. Settings of factorial design for the three experiments near Cairo.

Symbol	Factor	(30°, 0°)		(30°, 20°)		(30°, 30°)		Additional Settings	
		Low	High	Low	High	Low	High		
A	G_{eff}	119.1	194.6	115.6	196.1	111.6	197	Taguchi Design	L12 (2^10)
B	T_A	14.43	29.47	14.43	29.47	14.43	29.47	# of Unique Runs	12
C	V_w	2.9	4.2	2.9	4.2	2.9	4.2	# of Blocks	1
D	Y_a	3.46	5.7	3.45	5.72	3.33	5.74	# of Replicates	1

Table 2. Settings of factorial design for the three experiments near Riyadh.

Symbol	Factor	(30°, 0°)		(30°, 20°)		(30°, 30°)		Additional Settings	
		Low	High	Low	High	Low	High		
A	G_{eff}	144.6	205.8	143.1	202.1	140.5	203.7	Taguchi Design	L12 (2^10)
B	T_A	14.5	38.2	14.5	38.2	14.5	38.2	# of Unique Runs	12
C	V_w	2	3.6	2	3.6	2	3.6	# of Blocks	1
D	Y_a	4.58	5.57	4.49	5.49	4.37	5.41	# of Replicates	1

2.3. Reliability Analysis

In this major step, we proposed to use reliability engineering to predict some measurements to assess the PV system based on the information obtained from the simulation and factorial design steps. According to the IEEE standards, reliability engineering is a part of systems engineering that predicts the ability of the system to function properly for a specified time. Availability, maintainability, testability and maintenance are commonly

defined as parts of reliability engineering [20]. In other words, reliability is the probability of a system failure to occur after a specified time.

In systems engineering, the time of failure T is used as the random variable upon which the reliability analysis is based. To obtain a mathematical expression of reliability, we must have a probability distribution of the time of failure T (as a random event) to occur. The probability distribution function (pdf) is a function of time t that gives the probability of the time of failure (T) to occur or how probable the failure is to occur at a specified time [21]. As a probability function, $f(t)$ satisfies:

$$\int_{-\infty}^{\infty} f(t)dt \; = \; 1$$

In case of non-availability of data about the time of failure T, a distribution about the time of the system response can be used for this purpose. The change of any system response with time actually contains information about the success and failure of the system and their times. Thus, it is feasible to use the probability distribution function of the time of acceptable system response to predict the reliability of the system functionality. If the random variable T is the time after which the system response starts to be under an acceptable level and $f(t)$ is its pdf, then the cumulative probability density function $F(t)$ is defined as the probability of T to occur before time t. This function $F(t)$ is used to indicate the successful response of the system and is given by:

$$F(t) \; = \; P\,(T \; \leq \; t) = \int_{-\infty}^{t} f(k)dk$$

Since the reliability function $R(t)$ is the probability of T while the system is working successfully after time t, it is given by:

$$R(t) = 1 \; - \; F(t) = 1 - \int_{-\infty}^{t} f(k)dk$$

$$R(t) \; = \; \int_{t}^{\infty} f(k)dk \tag{4}$$

From (4), the following statistics can be calculated for assessment purposes:

Reliable life: the time to which a specified reliability x can still be achieved. It is calculated by solving $R(t) \; = \; x$ to obtain t. For example, the time at which a reliability of 90% can still be achieved is mathematically expressed by:

$$Reliable\_Life \; = \; (t|R(t) \; = \; x)\; Month \tag{5}$$

Mean life: the average time before failure of the unrepairable systems (or average time between consecutive failures for repairable system). Thus, the mean life is the time at which the reliability decays to the minimum acceptable reliability y. Thus,

$$Mean\_Life \; = \; (t|R(t) \; = \; y)\; Month \tag{6}$$

Failure rate: the reciprocal of the mean life. Thus,

$$Faliure\_Rate \; = \; \frac{1}{Mean\; Life}\; Month^{-1} \tag{7}$$

The system response that depends on more inputs and device factors can be used for the reliability study to predict the optimal usage of the system. In this work, we used the ReliaSoft Weibull++ software to predict $R(t)$, reliable life, mean life and failure rate of the system based on the pdf of the time of a selected system response. The data of the chosen system response collected from the simulation step were fed into the ReliaSoft Weibull++ software to process and fit it into a mathematical formula as an estimate of $f(t)$. The method

set to the software to estimate $f(t)$ and its parameters is the rank regression method (RRM). To determine how well the parameters of the estimated distribution fit the data, a goodness-of-fit (GOF) was used. This GOF utility uses three different statistical tests for this purpose. From the estimated function (t), the reliability function $R(t)$, $Reliable\_Life$, $Mean\_Life$ and $Failure\_Rate$ can be obtained according to Equations (4)–(7), respectively.

3. Results and Discussion

In this section, the results obtained after running the six experiments (three for each geographical region) are presented and discussed to draw a conclusion.

3.1. Results of Simulation Step

The changes of T_A and V_W over the 12 months are exactly the same for the three experiments of a geographical region but differ between the two regions, which can be observed in Figure 1b,c. The values G_{eff} vary from one experiment to another since they depend on the location and field orientation as shown in Figure 1a. G_{eff} shows smooth variation for the near Cairo but some irregular variation for the near Riyadh region. The obtained values of the array yield Y_a are plotted in Figure 2, which shows increased values during the summer months following an increase in the effective global irradiation. The smoothness and irregularity of G_{eff} are reflected in the array yield but in a nonlinear fashion. This nonlinearity may be due to the dusty weather in late autumn and the start of summer in Riyadh and mid-autumn in Cairo [22]. The array yield also shows variability among the three orientations during the cold months in both regions.

Figure 1. Inputs of the PV system over the 12 months for three orientations of the two regions. (**a**) Global effective radiation over the 12 months. (**b**) Ambient temperature over the 12 months (**c**) Velocity of wind over the 12 months.

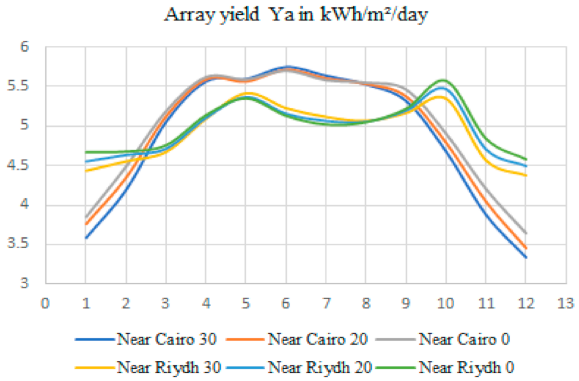

Figure 2. Array yield over the 12 months for three orientations of the two regions.

The PV system efficiency is shown in Figure 3, which demonstrates decreased efficiency during the summer months for both regions, which is expected due to the increased ambient temperature. The temperature for this time ranges from 25 to 29.5 °C near Cairo and from 34.7 to 39 °C near Riyadh. The minimum PV system efficiency is noted in mid-July when the temperature is at its maximum value, as shown in Figures 1b and 3. The lower efficiency of the system in the near Riyadh region confirms this conclusion, as the temperature in Riyadh is always higher than that in Cairo. Figure 3 also demonstrates variation of the system efficiency among the three orientations during the winter months in Cairo but no variation for that of Riyadh. This may be due to the fact that Riyadh is closer to the equator than Cairo, decreasing the effect of varying orientation.

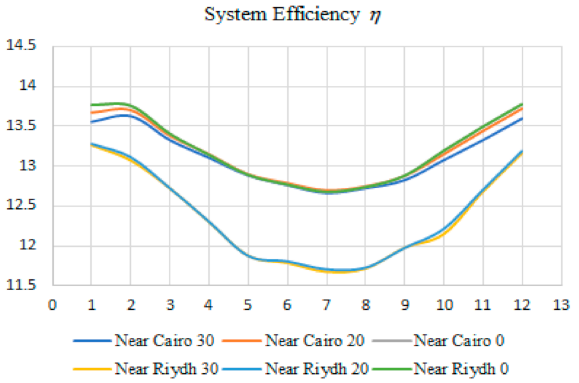

Figure 3. Efficiency of the PV system calculated over the 12 months for three orientations of the two regions.

Investigating Figure 4, the same description of PV system efficiency is noted for the PV system performance ratio, with increased variability among the three orientations for Cairo in the cold months.

The energy produced by the system over the 12 months changes in a fashion similar to those of the effective global radiation and the array yield as shown in Figure 5. Although there is decreased PV system efficiency and performance ratio during the summer months, the produced energy increases because of the increased effective global radiation. It is clear that the produced energy is higher in Cairo than in Riyadh for the three orientations, although there is less effective global radiation in Cairo. This is due to less temperature and cooling provided by the higher wind velocity in Cairo.

3.2. Results of Factorial Design Experiments

The Taguchi OA factorial design experiments showed the dependency of the responses on the factors and the significance of such a dependency. The software DOE++ provided the

results in different formats, from which we studied the significance of the factors based on their p_values and the equations describing the dependency of the responses on the factors.

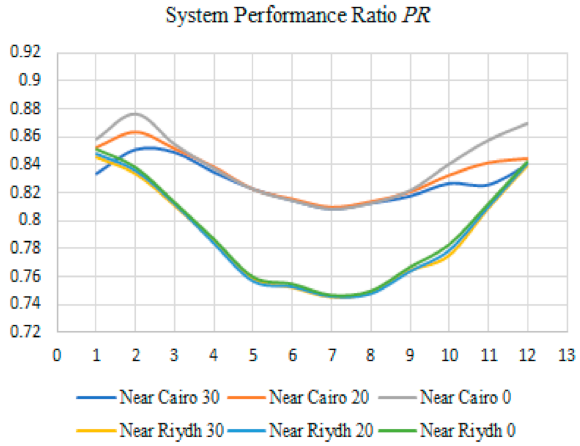

Figure 4. System performance ratio of the PV system calculated over the 12 months for three orientations of the two regions.

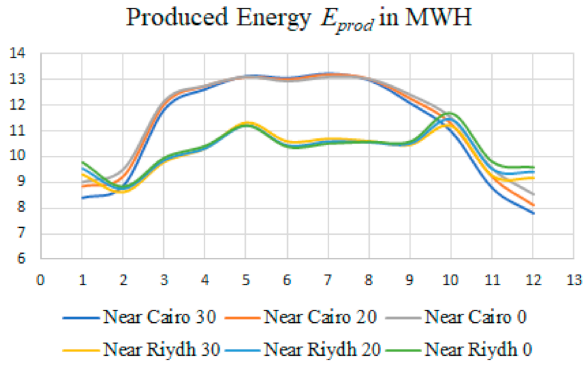

Figure 5. Energy produced by the PV system and available for usage over the 12 months for three orientations of the two regions.

The significance of each of the four factors (G_{eff}, T_A, V_w, Y_a) and their combinations is given in percentages such that:

$$significance = (1 - p\_value) * 100\%$$

The most significant factors and their levels of significance on the three responses (η, PR, E_{prod}) are presented in Tables 3 and 4 for near Cairo and near Riyadh, respectively.

Table 3. Most significant factors on the three responses for the three orientations near the Cairo region.

Response	Azimuth 0	Azimuth 20	Azimuth 30
η	T_A (81.5%)	T_A (90.5%)	T_A (73%)
PR	T_A Y_a (90%)	G_{eff} Y_a (96%)	G_{eff} Y_a (80%)
E_{prod}	G_{eff} (99%)	G_{eff} (92%)	G_{eff} (95%)

From Tables 3 and 4, the PV system efficiency η depends mostly on the ambient temperature for the two regions and the three field orientations. This result confirms the discussion provided above for the lower system efficiency in the near Riyadh region than that in the near Cairo region.

Table 4. Most significant factors on the three responses for the three orientations near the Cairo region.

Response	Azimuth 0	Azimuth 20	Azimuth 30
η	T_A (97%)	T_A (90.8%)	T_A (90%)
PR	T_A (97%)	T_A (95%)	T_A Y_a (94%)
E_{prod}	G_{eff} (99%)	G_{eff} (99%)	Y_a (100%)

In addition, from Tables 3 and 4, the energy produced by the system and available for usage E_{prod} is mostly affected by the global effective radiation G_{eff} and the array yield Y_a, which is actually related to G_{eff}.

However, the most significant factors on the PV system performance ratio PR varies from one region to the other and from field one orientation to the other. For this variability, the performance ratio is chosen to be used for the reliability study to predict the lifetime of the PV system at both regions with the three different field orientations.

Some of results obtained from the factorial design experiments to form the equations are shown in Table 3. A response is given by the summation of the obtained absolute value and the factors multiplied by the obtained coefficients. This table shows the coefficients of the factors and their combinations obtained for the field orientation ($30^\circ, 0^\circ$) of both regions. From this table, the PV system efficiency in near the Riyadh region at field orientation ($30^\circ, 0^\circ$) is given by:

$$\eta = 12.4241 \; + \; -0.7815 T_A \; + \; +0.0709 V_w \; + \; +0.0434 Y_a \; + \; +0.0409 G_{eff} \cdot T_A + \ldots$$

The most significant factors are highlighted in Table 5, which confirms the results obtained based on the p values.

Table 5. Some of the equations describing the responses with the most significant coefficients and factors highlighted.

	η = **13.3811+**		E_{prod} = **1.1059E + 04+**		PR = **0.8502+**	
Experiment 1 (Tilt 30°, Azimuth 0°) near Ciro	−0.2281	A: G_{eff}	**+2486.317**	**A:** G_{eff}	**−0.0309**	**A:** G_{eff}
	−0.2611	**B:** T_A	−81.3172	B: T_A	−0.0086	B: T_A
	+0.0289	C: V_w	+45.7601	C: V_w	−0.0036	C: V_w
	−0.1130	D: Y_a	−133.7523	D: Y_a	+0.0110	D: Y_a
	−0.0281	A • B	+188.7870	A • B	+0.0117	A • B
	−0.5774	A • C	−1122.8300	A • C	−0.0675	A • C
	+0.2379	A • D	+500.5546	A • D	+0.0469	A • D
	+0.2507	B • C	+651.1375	B • C	+0.0451	B • C
	−0.3359	B • D	−966.1647	B • D	−0.0739	B • D
	+0.2544	C • D	+510.0046	C • D	+0.0211	C • D
	η = **12.4241+**		E_{prod} = **9029.7552**		PR = **0.7924+**	
Experiment 2 (Tilt 30°, Azimuth 0°) near Riyadh	**−0.7815**	**B:** T_A	**+2331.782**	**A:**G_{eff}	+0.001	A: G_{eff}
	+0.0709	C: V_w	−586.0669	B: T_A	**−0.0500**	**B:** T_A
	+0.0434	D: Y_a	+252.3049	C: V_w	+0.0056	C: V_w
	+0.0409	A • B	+63.9783	D: Y_a	+0.0029	D: Y_a
	−0.1061	A • C	−37.6190	A • B	+0.0034	A • B
	−0.1565	A • D	−185.6370	A • C	−0.0093	A • C
	+0.0379	B • C	−197.7907	A • D	−0.0103	A • D
	+0.1881	B • D	−50.8167	B • C	+0.0031	B • C
	−0.0786	C • D	+98.3479	B • D	+0.0123	B • D
			−25.3812	C • D	−0.0039	C • D

3.3. Results of Reliability Analysis

Based on the results obtained from the simulation experiments, the PV system efficiency depends mainly on the ambient temperature, and the produced energy depends mainly on the global effective radiation. However, the PV system performance ratio (PR) depends on multiple factors. Thus, PR is the PV system response selected for reliability analysis.

The ReliaSoft Weibull++ software estimated a probability density function of PR with time $f(t)$ to be an exponential function given by:

$$f(t) = \lambda e^{-\lambda(t-\gamma)},\ f(t) \geq 0,\ \lambda > 0, t \geq \gamma \tag{8}$$

While the scale parameter λ indicates the stretch of the curve along the time axis, the location parameter γ idicates the shift of the curve from the origin. For exponential pdf, λ is related to γ by:

$$\lambda = \frac{1}{m-\gamma} \tag{9}$$

where t is the operating time (or life) and $(m-\gamma)$ is the mean of the pdf [21].

From Equations (4) and (8), $R(t)$ is given by:

$$R(t) = \int_t^\infty \lambda e^{-\lambda(k-\gamma)} dk$$

$$R(t) = e^{-\lambda(t-\gamma)}$$

Substitute for λ from Equation (9),

$$R(t) = e^{-\frac{(t-\gamma)}{(m-\gamma)}} \tag{10}$$

For experiment 1 (30°, 0°) and experiment 2 (30°, 20°) of the near Cairo region, the obtained value of the parameter γ is zero, and hence, the pdf is called the 1-paramter (1-p) distribution, and the corresponding reliability function is given by:

$$R(t) = e^{-\frac{t}{m}}$$

However, for the location parameter, $\gamma = 1$ for the remaining four experiments. Thus, the distribution is a 2-p distribution, and the corresponding reliability function $R(t)$ is given by:

$$R(t) = e^{\frac{-(t-1)}{(m-1)}}$$

- The reliability functions $R(t)$ of the PV system performance ratio for the six experiments are shown in Figure 6 with an assumed target reliability of 90%, indicated by the red horizontal line.
- As an example, the reliability at time $t = 100$ months is given in the first row of Tables 6 and 7 for the two regions. This value is greater for near Cairo for the two experiments (azimuth angles 0°, 20°), while it is greater for near Riyadh for the remaining experiments.
- The values of the $Mean\_Life$ are shown in the second row of Tables 6 and 7 for the two regions. The obtained $Mean\_Life$ values of the near Cairo region are 768.4, 772.2 and 659.4 months for experiments 1, 2 and 3, while those of near Riyadh are 685.63, 687.59 and 688.36, respectively. Thus, the field orientation (30°, 20°) gives the longest time for the near Cairo region, and the field orientation (30°, 30°) gives the longest lifetime for the near Riyadh region. The lifetimes of the systems in near Cairo are longer for orientations (30°, 0°) and (30°, 20°), while that of near Riyadh is longer for orientation (30°, 30°).

- The $Failure\_Rate$ equals the reciprocal of the $Mean\_Life$. The failure rate is given by the parameter λ, and the exact values are shown in the third row of Tables 6 and 7 for both regions.
- If we consider an acceptable limit of reliability to be 90%, then the $Reliable\_Life$ for the six experiments are less than their $Mean\_Life$ as shown in the fourth row of Tables 6 and 7. This result is logic as the reliability at the $Mean\_Life$ is usually much less than 90%. Considering a reliability of 50%, the system may have working reliably for 532.63, 535.28 and 457.38 months for the three orientations in the near Cairo region as shown in the fifth row of Table 6. This also shows that the field orientation (30°, 20°) is the best among the three orientations for near Cairo, as mentioned above, as it gives the longest time for a 50% reliability of the performance ratio. For a reliability of 50%, the system may have working reliably for 476.244, 477.605 and 564.470 months for the three orientations in the near Riyadh region as shown in the fifth row of Table 7. In addition, the field orientation (30°, 30°) is the best among the three orientations for near Riyadh, as mentioned above, as it gives the longest time for the 50% reliability of the performance ratio.

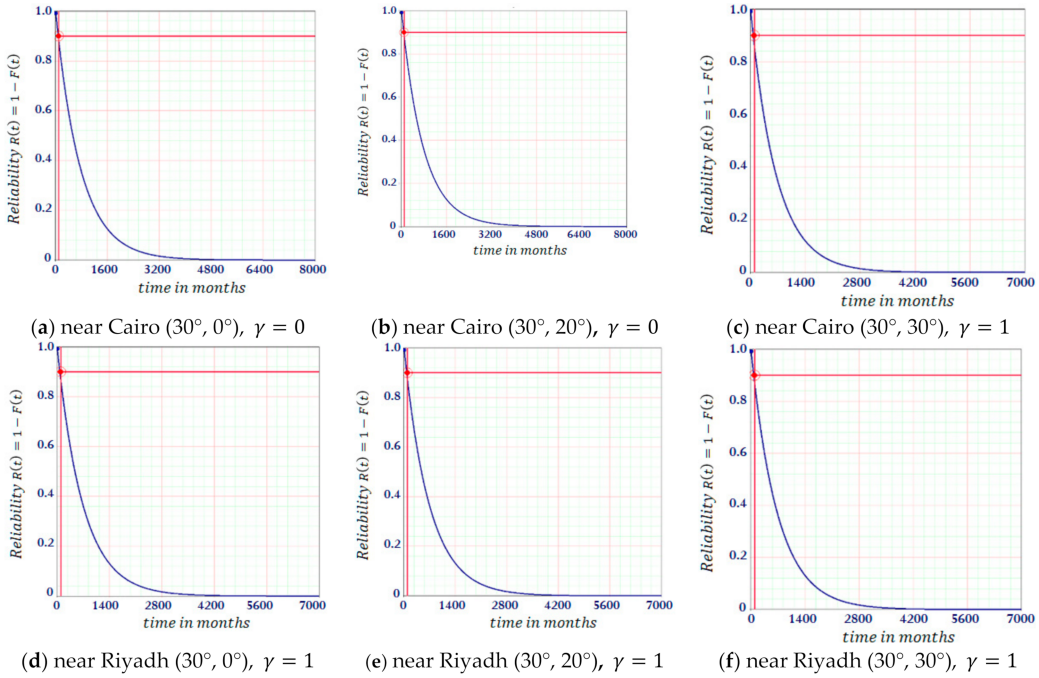

Figure 6. The reliability functions $R(t)$ of: (**a**,**d**) field orientation (30° tilt, 0° azimuth), (**b**,**e**) field orientation (30° tilt, 20° azimuth) and (**c**,**f**) field orientation (30° tilt, 30° azimuth).

Table 6. Results obtained by the reliability analysis for the near Cairo region.

Statistic	30° Tilt, 0° Azimuth	30° Tilt, 20° Azimuth	30° Tilt, 30° Azimuth
$R\ (t = 100)$	0.877977	0.878542	0.860399
$Mean\_Life$	768.43 months	772.25 months	658.42 months
$Failure\_Rate$	0.001301/months	0.001295/months	0.001519/months
$Reliable\_Life: (t\|R = 0.9)$	80.96 months	81.36 months	70.37 months
$Reliable\_Life: (t\|R = 0.5)$	532.63 months	535.28 months	457.38 months

Table 7. Results obtained by the reliability analysis for the near Riyadh region.

Statistic	30° Tilt, 0° Azimuth	30° Tilt, 20° Azimuth	30° Tilt, 30° Azimuth
$R\ (t = 100)$	0.865548	0.865905	0.884444
$Mean\_Life$	685.63 months	687.59 months	688.36 months
$Failure\_Rate$	0.001459/months	0.001454/months	0.001228/months
$Reliable\_Life:\ (t \vert R = 0.9\ )$	73.238 months	73.455 months	85.801 months
$Reliable\_Life:\ (t \vert R = 0.5)$	476.244 months	477.605 months	564.470 months

4. Conclusions

In conclusion, this work proposed a method to predict some statistics to assess the quality of the PV systems. To achieve this goal, data collected from two different geographical regions were used to simulate the PV system work. The simulation results showed that the higher the temperature, the lower the PV system efficiency. This is valid for the change of temperature along the year and among different locations.

From the collected inputs, obtained device factors and system responses, the most comprehensive variables were selected to undergo a Taguchi OA experiment to obtain the dependency of the system responses on the inputs and device factors. This algorithm obtained the level of significance of each of the inputs and devised factors on the system responses. In turn, it helped to choose the best system response that could be used for reliability analysis. The Taguchi OA showed that the PV system efficiency and the produced energy are highly dependent on the ambient temperature and the global effective radiation, respectively. It also revealed that the performance ratio of the PV system varies with many inputs and device parameters, which makes it a reliability analysis candidate.

The reliability analysis applied to the performance ratio of the PV system showed that the field orientation (30°, 20°) leads to the longest lifetime of the PV system in the near Cairo region, while the field orientation (30°, 30°) leads to the longest lifetime of the PV system in the near Riyadh region.

Author Contributions: Conceptualization, N.S. and A.E.B.; methodology, N.S.; software, A.E.B.; validation, A.E.B.; formal analysis, N.S.; investigation, N.S.; resources, A.E.B.; writing—original draft preparation, N.S.; writing—review and editing, N.S.; visualization, N.S.; supervision, N.S.; project administration, N.S.; funding acquisition, N.S. All authors have read and agreed to the published version of the manuscript.

Funding: This work was supported by the Deanship of Scientific Research, King Faisal University, United Arab Emirates (grant number NA000138).

Institutional Review Board Statement: Not applicable.

Informed Consent Statement: Not applicable.

Data Availability Statement: The reported data-supporting results can be found at this link. The input data presented in this link are read by the software PVsyst from the databases. However, we cannot access the database itself. All simulation data and the results can be found here. https://drive.google.com/drive/folders/1PGB4dzEkn7lVHH7xW2pndeWybn3kYGVc (accessed on 8 February 2022).

Acknowledgments: The authors extend their appreciation to the Deputyship for Research and Innovation, Ministry of Education in Saudi Arabia for funding this research work through project number NA000138.

Conflicts of Interest: The authors declare no conflict of interest.

References

1. Bergmann, E.A.; Colombo, S.; Hanley, N. The Social-Environmental Impacts of Renewable Energy Expansion in Scotland. In Proceedings of the Agricultural Economics Society's 81st Annual Conference, Reading, UK, 2–4 April 2007; University of Reading: Reading, UK, 2007; Volume 81, pp. 1–33.
2. MacKay, D.J.C. Solar energy in the context of energy use, energy transportation and energy storage. *Philos. Trans. R. Soc.* **2013**, *371*, 20110431. [CrossRef] [PubMed]
3. Lee, M.M.; Teuscher, J.; Miyasaka, T.; Murakami, T.N.; Snaith, H.J. Efficient Hybrid Solar Cells Based on Meso-Superstructured Organometal Halide Perovskites. *Science* **2012**, *338*, 643–647. [CrossRef] [PubMed]
4. Bouich, A.; Mari, B.; Atourki, L.; Ullah, S.; Touhami, M.E. Shedding Light on the Effect of Diethyl Ether Antisolvent on the Growth of (CH_3NH_3) PbI_3 Thin Films. *JOM Miner. Met. Mater. Soc.* **2021**, *73*, 551–557. [CrossRef]
5. Bouich, A.; Marí-Guaita, J.; Bouich, A.; Pradas, I.G.; Marí, B. Towards Manufacture Stable Lead Perovskite APbI3 (A = Cs, MA, FA) Based Solar Cells with Low-Cost Techniques. *Eng. Proc.* **2022**, *12*, 81. [CrossRef]
6. Ravi, R.; Manoj, K.; Brijesh, T. Solar Photovoltaic System Design Optimization by Shading Analysis to Maximize Energy Generation from Limited Urban Area. *Energy Convers. Manag.* **2016**, *115*, 244–252.
7. Li, D.H.; Lou, S.; Lam, J.C. An Analysis of Global, Direct and Diffuse Solar Radiation. *Energy Procedia* **2015**, *75*, 388–393. [CrossRef]
8. Elyaqouti, M.; Lahoussine, B.; Ahmed, I. Global Solar Radiation Estimation on a Horizontal and Tilted Plane in Agadir City, Morocco. *Int. J. Comput. Appl.* **2016**, *137*, 21–24. [CrossRef]
9. Seyed, A.M.M.; Hashim, H.; Chandima, G. Estimation of Hourly, Daily and Monthly Global Solar Radiation on Inclined Surfaces: Models Re-Visited. *Energies* **2017**, *10*, 134.
10. Maatallah, T.; El Alimi, S.; Nassrallah, S.B. Performance modeling and investigation of fixed, single and dual-axis tracking photovoltaic panel in Monastir city, Tunisia. *Renew. Sustain. Energy Rev.* **2011**, *15*, 4053–4066. [CrossRef]
11. Mohsen, F.; Mohd, A.M.R.; Mohammad, F.; Mahdi, Z.; Zohreh, G. Optimization and comparison analysis for application of PV panels in three villages. *Energy Sci. Eng.* **2015**, *3*, 145–152.
12. Özgür, Ç.; Ahmet, T.; Yıldırım, H.B. The optimized artificial neural network model with Levenberg–Marquardt algorithm for global solar radiation estimation in Eastern Mediterranean Region of Turkey. *J. Clean. Prod.* **2016**, *116*, 1–12.
13. Ogbonnaya, C.; Turan, A.; Abeykoon, C. Robust code-based modeling approach for advanced photovoltaics of the future. *Sol. Energy* **2020**, *199*, 521–529. [CrossRef]
14. Kasra, M.; Shahabuddin, S.; AmirRudin, K.; Lai, P.C.; Zulkefli, M. Identifying the most significant input parameters for predicting global solar radiation using an ANFIS selection procedure. *Renew. Sustain. Energy Rev.* **2016**, *63*, 423–434.
15. Premalatha, N.; Valan Arasu, A. Prediction of solar radiation for solar systems by using ANN models with different back propagation algorithms. *J. Appl. Res. Technol.* **2016**, *14*, 206–214. [CrossRef]
16. Al-Dahidi, S.; Osama, A.; Jehad, A.; Mohamed, L. Assessment of Artificial Neural Networks Learning Algorithms and Training Datasets for Solar Photovoltaic Power Production Prediction. *Front. Energy Res.* **2019**, *7*, 130. [CrossRef]
17. Wang, J.; Xie, Y.; Zhu, C.; Xu, X. Daily solar radiation prediction based on Genetic Algorithm Optimization of wavelet neural network. In Proceedings of the 2011 International Conference on Electrical and Control Engineering ICECE, Yichang, China, 16–18 September 2011; pp. 602–605.
18. Hossein, K.; Kasra, M.; Mahdi, J. A statistical comparative study to demonstrate the merit of day of the year-based models for estimation of horizontal global solar radiation. *Energy Convers. Manag.* **2014**, *87*, 37–47.
19. Kacker, R.N.; Lagergren, E.S.; Filliben, J.J. Taguchi's Orthogonal Arrays Are Classical Designs of Experiments. *J. Res. Natl. Inst. Stand. Technol.* **1991**, *96*, 577–591. [CrossRef] [PubMed]
20. Brauer, D.C.; Brauer, G.D. Reliability-Centered Maintenance. *IEEE Trans. Reliab.* **1987**, *R-36*, 17–24. [CrossRef]
21. O'Connor, A.N.; Modarres, M.; Mosleh, A. *Distribution Function in Probability Distributions Used in Reliability Engineering*; Center for Reliability Engineering, University of Maryland: College Park, MD, USA, 2016; pp. 9–19.
22. Shahin, M. Climate of the Arab Region. In *Water Resources and Hydrometeorology of the Arab Region*; Springer: Cham, Switzerland, 2007; Chapter 3; pp. 77–134.